EVIDENCE OF RING-FAULTS IN ORIENTALE FROM GRAVITY. Y. N. Kattoum[1] and J. C. Andrews-Hanna, [1]Department of Geophysics, Colorado School of Mines, Golden, CO, ykattoum@mines.edu, jcahanna@mines.edu

Introduction: The Orientale basin has long been of interest for its well-preserved multi-ring basin structure. It consists of three concentric ring structures known as the Inner Rook (R=230 km), Outer Rook (R=350 km), and Cordillera (R=490 km) (Figure 1a). Based on geologic evidence, the Cordillera mountains have been interpreted as forming through listric normal faulting from the inward collapse of the interior basin [1]. A similar mechanism may have been responsible for the formation of the Outer Rook, though it has also been described as the rim corresponding to the collapsed excavation cavity. We here examine the internal crustal structure of Orientale to determine the existence and geometry of the ring faults. This information has important implications for multi-ring basin formation and modification. Additionally, it can also help aid in predicting what kind of information can be extracted from anticipated higher resolution gravity coming from GRAIL.

Method: Previous studies of basin structure have focused primarily on spherical harmonic analyses [2]. However, discrete structures such as faults cannot be adequately represented using spherical harmonic functions. Thus, we here take a forward approach, modeling the gravity anomalies arising from ring faults of assumed geometry for comparison with the gravity data. As the ring faults cross density interfaces in the subsurface, the offsets across those interfaces will generate gravity anomalies that can be measured at the surface. In order to isolate the subsurface effects of the basin structure, the Bouguer anomaly is calculated [3] (Figure 1b) from the gravity data [4]. The Bouguer anomaly was calculated up to degree 120 with a cosine taper from degree 100-120 to dampen high frequency noise. Degrees 2,0 and 2,2 were removed to account for rotational-tidal deformation [3]. Orientale was than isolated from the global map by averaging a set of radial profiles extending outward from the center of the basin with an azimuthal spacing of 3°, which has the effect of amplifying the signal to noise ratio allowing for a higher resolution analysis [6].

A series of 3D gravity forward models were then calculated using rectangular prisms [5] to represent the internal structure of the basin. Since the Moon is believed to have a dual-layered crust consisting of an anorthositic upper crust and a noritic lower crust [2], a dual-layered crustal model is employed. The model included an intracrustal interface and a crust-mantle interface or Moho with horizontal prism dimensions of

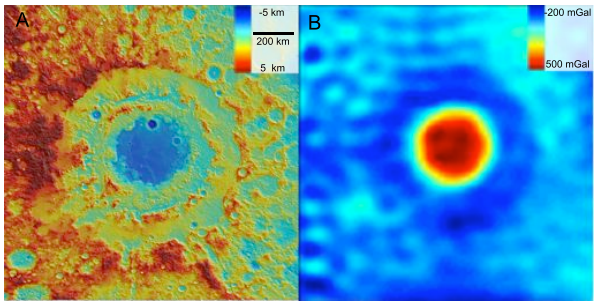

Figure 1: A) Topography of Orientale Basin overlain on shade of relief map. B) The Bouguer anomaly of Orientale.

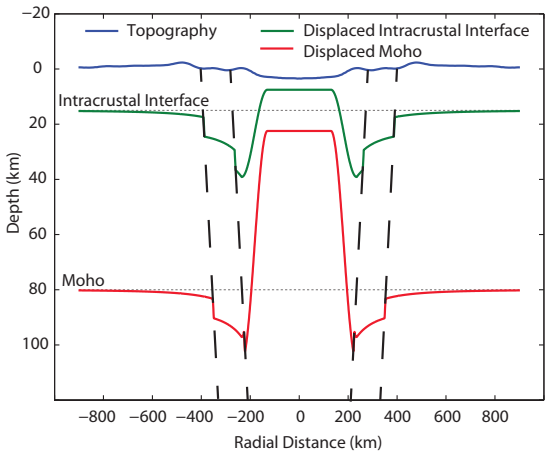

Figure 2: Model cross section of subsurface of Orientale. Oblique dashed lines represent 60º faults with vertical displacement of 7 km.

1 km (Figure 2). The large positive Bouguer anomaly observed in the center of Orientale is believed to be associated with an uplifted mantle plug [6], so this is matched with an uplifted Moho and intracustal interface in the models. Additionally, the negative anomalies outside the basin center are thought to be a result of crustal thickening that arises from the ejecta deposits, resulting in a downward displacement of the Moho. The thickness of the ejecta [7] is used to approximate the crustal thickening outside the basin, with the excess crust applied to the upper crust only. With the two interfaces in place, two normal faults are then created at the rings. The Cordillera fault is assumed to intersect the surface at the lower flank of the Cordillera Mountains with the Outer Rook Fault following a similar manner. The two faults generate displacements across the intracrustal interface and Moho, with the location and magnitude of the offsets determined by the assumed dip and displacement on the faults.

In order to ensure that the model results can be fairly compared with the data, the model Bouguer anomaly was calculated at a height of 3 km and processed using the same procedure applied to the data. Hence, the model results are expanded into spherical harmonics to the same degree on a global grid and radial profiles are taken out from the model center and azimuthally averaged. Since the effect of the faults in the Bouguer anomaly is subtle, the first horizontal derivative is taken for both the data and the model results ($\partial g_B/\partial r$, where r is the radial direction from the center of the basin). The first derivative of the gravity anomaly is commonly used in the technique of gravity gradiometry to isolate the boundaries of density contrasts as can arise at faults. A moving average filter was then employed to smooth out the noise.

A series of parameters that include the depth to the intracrustal interface, lower crustal density, fault displacement, and fault dip are then explored to match the data. The nominal densities used for the upper crust (2800 kg/m^3), lower crust (3100 kg/m^3), and mantle (3400 kg/m^3) were chosen based on the suggested mineralogy of these layers [3]. A model with 60° dip faults, 7 km fault displacements, and an intracustal interface depth of 15 km with the nominal densities is chosen to be the default model. From this model the parameters are varied one at a time to explore their effects. Fault displacements of 3, 5, and 7 km for the Cordillera and Outer Rook Fault were chosen based on the ~3-7 km observed displacement of the ring scarps in the topography. Fault dips of 20°, 40°, 60°, and 80° were considered. Finally, depths to the intracrustal interface of 15, 30, and 45 km were considered.

Results: The horizontal gradient of the observed Bouguer anomaly shows distinctive patterns around the basin (Figure 3a, bold line). A strong negative gradient is observed, corresponding to the edge of the uplifted mantle plug. The Bouguer gradient then flattens out in a shelf at the basin rim, followed by a small positive bump. Qualitatively, this positive Bouguer gradient anomaly is consistent with the expectations for an inward facing scarp offsetting a density interface separating a lower density layer above from a higher density layer below.

While models lacking ring faults did not display the observed shelf and hump, all models with faults exhibited variations of this structure. For example, greater fault displacements produced larger magnitudes in the shelf and bump (Figure 3a). On the other hand, shallower dips shifted the bump slightly downward and then inward toward the center of the basin (Figure 3b). Finally, the variations of intracrustal depth produce broader bumps and less distinct shelves as the intracrustal depth was increased (Figure 3c).

Conclusion: Evidence of faulting within Orientale is seen in the current gravity data. The parameters that best represented the fault signatures in the observed Bouguer gravity gradient were 40º faults with a displacement of 7 km, intersecting an intracrustal interface at 15 km depth (Figure 2b). The fault dip of 40º is consistent with a listric normal fault with decreasing dip at depth. The fault displacements in the models are also consistent in what is seen in the topography, with observed displacements of up to ~7 km between the Cordillera and the Outer Rook and ~7 between the Outer Rook and Inner Rook. Future analyses with the anticipated GRAIL data will more tightly constrain the internal structure of Orientale and its rings.

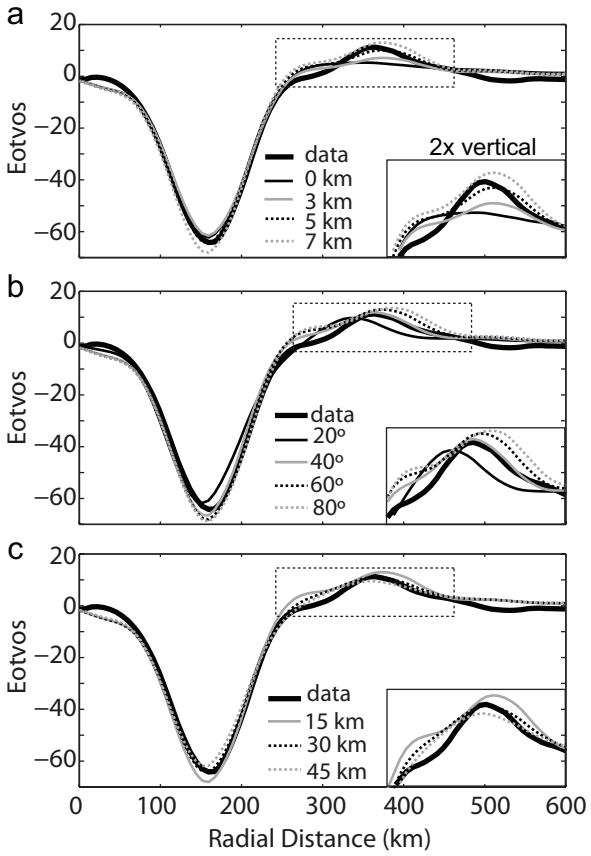

Figure 3*:* a) Horizontal gradient of Bouguer anomaly of Orientale and models with different fault displacements. b) Data an models with different fault dips. c) Data and model with varying intracrustal interface depths.

References: [1] Head, J. W. (2010),*GRL*, *37*, 5, doi: 201010.1029/2009GL041790. [2] Wieczorek, M. A., and R. J. Phillips (1999), *Icarus*, *139*, 246-259. [3] Wieczorek, M. A., and R. J. Phillips (1998), *JGR*, *103*, 1715. [4] Mazarico, E., F. G. Lemoine, S.-C. Han, and D. E. Smith (2010), *JGR* , *115*, 14, doi: 201010.1029/2009JE003472. [5] Blakely, R. J. (1996), Cambridge University Press. [6] Andrews-Hanna J.C., S.T. Stewart, (2011) LPSC XLII, 2194. [7] Fassett, C. I., J. W. Head, D. E. Smith, M. T. Zuber, and G. A. Neumann (2011), *GRL*, *38*, 17201.